# Disk Formation Mechanisms

♣ Rotationally supported circumstellar disks evidently originate in the collapse of self-gravitating, rotating, molecular cloud cores.

⋆ Molecular line observations have established that a majority of dense ($\gtrsim 10^4\,\mathrm{cm}^{-3}$) cloud cores show evidence of rotation, with angular velocities $\sim 3\times10^{-15} - 10^{-13}\,\mathrm{s}^{-1}$ that tend to be uniform on scales of $\sim 0.1\,\mathrm{pc}$, and with specific angular momenta in the range $\sim 4\times10^{20} - 3\times10^{22}\,\mathrm{cm}^2\,\mathrm{s}^{-1}$.

⋆ The cores can transfer angular momentum to the ambient gas through magnetic braking, a process that also tends to align their angular velocity and large-scale magnetic field vectors on a dynamical timescale.

⋆ Once dynamical collapse is initiated and a core goes into a near–free-fall state, the specific angular momentum is expected to be approximately conserved, resulting in a progressive increase in the centrifugal force that eventually halts the collapse and gives rise to a rotationally supported disk on scales $\sim 10^2\,\mathrm{AU}$; this picture is consistent with interferometric molecular-line observations of contracting cloud cores.

# Modeling framework

Krasnopolsky & Königl (2002)

♣ Numerical simulations of magnetically supported clouds have demonstrated that the gas rapidly contracts along the field lines and maintains force equilibrium along the field even during the collapse phase, including in cases where the clouds are initially elongated in the field direction. This motivates treating the collapse as being quasi 1D.

♣ To obtain semi-analytic solutions, postulate self-similarity (in space and time; similarity variable $x \equiv r/Ct$, where $C$ is the isothermal speed of sound).

- ⋆ Core collapse is a multiscale problem, which is expected to assume a self-similar form away from the outer and inner boundaries and not too close to the onset time (e.g., Penston 1969; Larson 1969; Shu 1977; Hunter 1977). This has been verified by numerical and semianalytic treatments of restricted core-collapse problems – with/without rotation and with/without magnetic fields.

- ⋆ The necessary assumption of isothermality can be justified mainly by the fact that thermal stresses do not play a major role in the dynamics of the collapsing core.

♣ To account for the weak ionization of the cloud cores, incorporate ambipolar diffusion into the model.

⋆ The ion–neutral drift velocity is negligible after the start of the dynamical core-collapse phase. However, once the central mass begins to grow, ambipolar diffusion becomes important within the gravitational "sphere of influence" of the central mass: as the incoming matter decouples from the field and continues moving inward, the decooupling front moves outward and steepens into a C-type ambipolar diffusion shock (Ciolek & Königl 1998; Contopoulos et al. 1998; cf. Li & McKee 1996).

⋆ To incorporate ambipolar diffusion into the self-similarity formulation, it is necessary to adopt $\rho_i = \mathcal{K}\rho^{1/2}$. This approximation is applicable on both ends of a density range spanning $\sim 8$ orders of magnitude, which corresponds roughly to radial scales $\sim 10 - 10^4$ AU, with $\mathcal{K}$ varying by only 1 order of magnitude across this interval.

♣ The transition from a nearly freely falling, collapsing core to a quasi-stationary, rotationally supported disk involves a strong deceleration in a centrifugal shock. This shock is distinct from the ambipolar-diffusion shock mentioned above: it typically occurs at a different radius and is hydrodynamic, rather than hydromagnetic, in nature.

♣ To allow mass to accumulate at the center in a rotating-core collapse, an angular momentum transport mechanism must be present.

⋆ It is assumed that magnetic braking, the **vertical** tranport of angular momentum through torsional Alfvén waves, continues to operate also during this phase of the core evolution. To incorporate it into the self-similarity framework, one has to assume that $V_{\rm A,ext}$ (the Alfvén speed in the ambient medium) is a constant. (Note that in the ISM one in fact infers $V_{\rm A,ext} \approx {\rm const} \;\; \approx 1 \ {\rm km \ s^{-1}}$ in the density range $\sim 10^3 - 10^7 \ {\rm cm^{-3}}$.)

⋆ One can verify that magnetic braking dominates radial transport by MRI turbulence and gravitational torques in the derived solutions.

⋆ It is, however, also found that vertical angular momentum transport from the disk by a centrifugally driven wind arises naturally (and may dominate) for fiducial parameter values.

# Magnetized Isothermal Disk Equations

Mass

$$\frac{\partial \rho}{\partial t} + \frac{1}{r}\frac{\partial}{\partial r}(r\rho V_r) = -\frac{\partial}{\partial z}(\rho V_z) \ , \tag{33}$$

Radial Momentum

$$\rho\frac{\partial V_r}{\partial t}+\rho V_r\frac{\partial V_r}{\partial r} = \rho g_r - C^2\frac{\partial \rho}{\partial r}+\rho\frac{V_\phi^2}{r}+\frac{B_z}{4\pi}\frac{\partial B_r}{\partial z}-\frac{\partial}{\partial r}\left(\frac{B_z^2}{8\pi}\right)$$

$$-\frac{1}{8\pi r^2}\frac{\partial}{\partial r}(rB_\phi)^2-\rho V_z\frac{\partial V_r}{\partial z} \ , \tag{34}$$

Angular Momentum

$$\frac{\rho}{r}\frac{\partial}{\partial t}(rV_\phi) + \frac{\rho V_r}{r}\frac{\partial}{\partial r}(rV_\phi) = \frac{B_z}{4\pi}\frac{\partial B_\phi}{\partial z} + \frac{B_r}{4\pi r}\frac{\partial}{\partial r}(rB_\phi) - \rho V_z\frac{\partial}{\partial z}(rV_\phi) \ , \tag{35}$$

Vertical Momentum

$$C^2\frac{\partial \rho}{\partial z} = \rho g_z - \frac{\partial}{\partial z}\left(\frac{B_\phi^2}{8\pi}+\frac{B_r^2}{8\pi}\right) + \frac{B_r}{4\pi}\frac{\partial B_z}{\partial r} \ . \tag{36}$$

# Vertically Integrated Disk Equations

Thin-Disk approximation: $B_z = \text{const}$ (except in $\partial B_z/\partial z$ term); $B_r$ and $B_\phi$ increase $\propto z$; all terms $\mathcal{O}(H/r)$ (where $H$ is the disk half thickness) are neglected except in $[B_{r,\mathrm{s}} - H(\partial B_z/\partial r)]$.

Mass

$$\frac{\partial \Sigma}{\partial t} + \frac{1}{r}\frac{\partial}{\partial r}(r\Sigma V_r) = -\frac{1}{2\pi r}\frac{\partial \dot{M}_{\mathrm{w}}}{\partial r}\,, \qquad (37)$$

Radial Momentum

$$\frac{\partial V_r}{\partial t} + V_r\frac{\partial V_r}{\partial r} = g_r - \frac{C^2}{\Sigma}\frac{\partial \Sigma}{\partial r} + \frac{B_z}{2\pi\Sigma}\left(B_{r,\mathrm{s}} - H\frac{\partial B_z}{\partial r}\right) + \frac{J^2}{r^3}\,, \qquad (38)$$

Angular Momentum

$$\frac{\partial J}{\partial t} + V_r\frac{\partial J}{\partial r} = \frac{rB_zB_{\phi,\mathrm{s}}}{2\pi\Sigma}\,, \qquad (39)$$

Vertical Momentum

$$\frac{\Sigma C^2}{2H} = \frac{\pi}{2}G\Sigma^2 + \frac{GM_*\rho H^2}{2r^3} + \frac{1}{8\pi}\left(B_{\phi,\mathrm{s}}^2 + B_{r,\mathrm{s}}^2 - B_{r,\mathrm{s}}\,H\frac{\partial B_z}{\partial r}\right). \qquad (40)$$

## Magnetic Braking

$$B_{\phi,\mathrm{s}}(r) = -\frac{\Psi(r)}{\pi r^2}\left(\frac{V_{\mathrm{i},\phi}(r)}{V_{\mathrm{A,ext}}}\right) \tag{41}$$

(same as eq. [12] except that $V_\phi$ is replaced by $V_{\mathrm{i},\phi}$ to account for the fact that the field lines in the mostly neutral medium are anchored in the ionized component).

Ion equation of motion in ambipolar-diffusion limit

$$\rho\nu_{\mathrm{ni}}\mathbf{V}_{\mathrm{D}} = \frac{1}{4\pi}(\nabla\times\mathbf{B})\times\mathbf{B}\ , \tag{42}$$

where $\mathbf{V}_{\mathrm{D}} \equiv \mathbf{V}_{\mathrm{i}} - \mathbf{V}_{\mathrm{n}}$. In particular,
$V_{\mathrm{D},\phi} = B_z B_{\phi,\mathrm{s}}/2\pi\nu_{\mathrm{ni}}\Sigma$
$V_{\mathrm{D},r} = (B_z/2\pi\nu_{\mathrm{ni}}\Sigma)(B_{r,\mathrm{s}} - H\partial B_z/\partial r)$.

Expressing $V_{\mathrm{i}\phi}$ in eq. (41) in terms of $V_\phi$ and $V_{\mathrm{D},\phi}$ and imposing a cap ($\delta \lessapprox 1$) on $|B_{\phi,s}|/B_z$ (to account for the possible development of a kink instability above the disk surface), one gets

$$B_{\phi,s} = -\min\left[\frac{\Psi}{\pi r^2}\frac{V_\phi}{V_{\mathrm{A,ext}}}\left(1+\frac{\Psi B_z}{2\pi^2 r^2\nu_{\mathrm{ni}}\Sigma V_{\mathrm{A,ext}}}\right)^{-1}; \delta B_z\right]\ . \tag{43}$$

Flux conservation relation:

$$\frac{\partial \Psi}{\partial t} = -2\pi r V_{\mathrm{i},r} B_z = -2\pi r \left(V_r + V_{\mathrm{D},r}\right) B_z \ , \quad (44)$$

In the limit of a potential field ($\nabla \times \mathbf{B} = 0$) outside an infinitely thin disk, $B_{r,\mathrm{s}}(r)$ can be determined from an $r$-integral of the midplane value of $B_z$:

$$B_{r,\mathrm{s}} = \int_0^\infty dk \, J_1(kr) \int_0^\infty dr' r' [B_z(r' - B_{\mathrm{ref}}] J_0(kr') \quad (45)$$

(e.g., Ciolek & Mouschovias 1993), where $J_0$ and $J_1$ are Bessel functions of order 0 and 1, respectively, and $B_{\mathrm{ref}}$ is the uniform ambient field at "infinity" (which is henceforth neglected). A similar integral can be written for $g_r$ [over $\Sigma(r)$]. These integrals can be approximated by their monopole terms:

$$\begin{aligned} B_{r,s} &= \frac{\Psi(r,t)}{2\pi r^2} \ , \\ g_r &= -\frac{GM(r,t)}{r^2} \ . \end{aligned} \quad (46)$$

When $B_z(r)$ [resp. $\Sigma(r)$] scales as $r^{-q}$, one obtains the monopole expression for $B_{r,\mathrm{s}}$ (resp. $g_r$) with a coefficient $C(q) \sim \mathcal{O}(1)$ (Ciolek & Königl 1998).

## Self-similarity formulation

$$x = r/Ct \ ,$$

$$\begin{gathered} H(r,t) = Ct\, h(x)\,, \quad \Sigma(r,t) = (C/2\pi G t)\,\sigma(x) \ , \\ V_r(r,t) = C\, u(x)\,, \quad V_\phi(r,t) = C\, v(x) \ , \\ g_r(r,t) = (C/t)\, g(x)\,, \quad J(r,t) = C^2 t\, j(x) \ , \\ M(r,t) = (C^3 t/G)\, m(x)\,, \quad \dot{M}(r,t) = (C^3/G)\, \dot{m}(x) \ , \\ \mathbf{B}(r,t) = (C/G^{1/2} t)\, \mathbf{b}(x)\,, \Psi(r,t) = (2\pi C^3 t/G^{1/2})\psi(x) \ . \end{gathered}$$

Assumed vertical hydrostatic equilibrium ⇒ disk half-thickness $h$:

$$\left(\frac{\sigma m_c}{x^3} - b_{r,s}\frac{db_z}{dx}\right) h^2 + \left(b_{r,s}^2 + b_{\phi,s}^2 + \sigma^2\right) h - 2\sigma = 0$$

$$\Rightarrow \quad h = \frac{\hat{\sigma} x^3}{2\hat{m}_c}\left[-1 + \left(1 + \frac{8\hat{m}_c}{x^3\hat{\sigma}^2}\right)^{1/2}\right] \ ,$$

where $\hat{m}_* \equiv m_* - x^3 b_{r,s}(db_z/dx)/\sigma$ and $\hat{\sigma} \equiv \sigma + (b_{r,s}^2 + b_{\phi,s}^2)/\sigma$.

Initial Conditions (based on numerical simulations) correspond to structure just before point-mass formation:

$$\sigma \to \frac{A}{x},\ b_z \to \frac{\sigma}{\mu_0},\ u \to u_0,\ v \to v_0 \ \text{ as } x \to \infty\,,$$

with $A = 3,\ \mu_0 = 2.9,\ u_0 = -1.$

Solve as a boundary value problem using $x \to 0$ asymptotic behavior.

## Asymptotic behavior for circumstellar disks

$$
\begin{aligned}
\dot{m} &= m = m_* \ , \\
j &= m_*^{1/2} x^{1/2} \ , \\
-u &= w = (m_*/\sigma_1) x^{1/2} \ , \\
\sigma &= \frac{(2\eta/3\delta)(2m_*)^{1/2}}{[1+(2\eta/3\delta)^{-2}]^{1/2}} x^{-3/2} \\
&\equiv \sigma_1 \ x^{-3/2} \ , \\
b_z &= -b_{\phi,\mathrm{s}}/\delta = [m_*{}^{3/4}/(2\delta)^{1/2}] \ x^{-5/4} \ , \\
b_{r,\mathrm{s}} &= \psi/x^2 = (4/3) b_z \ , \\
h &= \{2/[1+(2\eta/3\delta)^2] m_*\}^{1/2} \ x^{3/2} \ .
\end{aligned}
$$

Vary $\delta = |B_{\phi,s}|/B_z$, $\alpha \equiv C/V_{\mathrm{A,ext}}$, $v_0 \equiv V_{\phi,0}/C$, and $\eta \equiv \tau_{\mathrm{ni}} \, (4\pi G \rho)^{1/2}$.

Fiducial Solution: $\eta = 1$, $v_0 = 0.73$, $\alpha = 0.08$, $\delta = 1$

Initial rotation is not very fast and the braking is moderate $\Rightarrow$ AD shock is located further away from the center than the centrifugal shock ($x_{\mathrm{a}}/x_{\mathrm{c}} \approx 30$).

For $C = 0.19 \ \mathrm{km \ s^{-1}}$,
$x = 1 \Leftrightarrow \{400, \ 4000\} \ \mathrm{AU}$ at $t = \{10^4, \ 10^5\} \ \mathrm{yr}$.

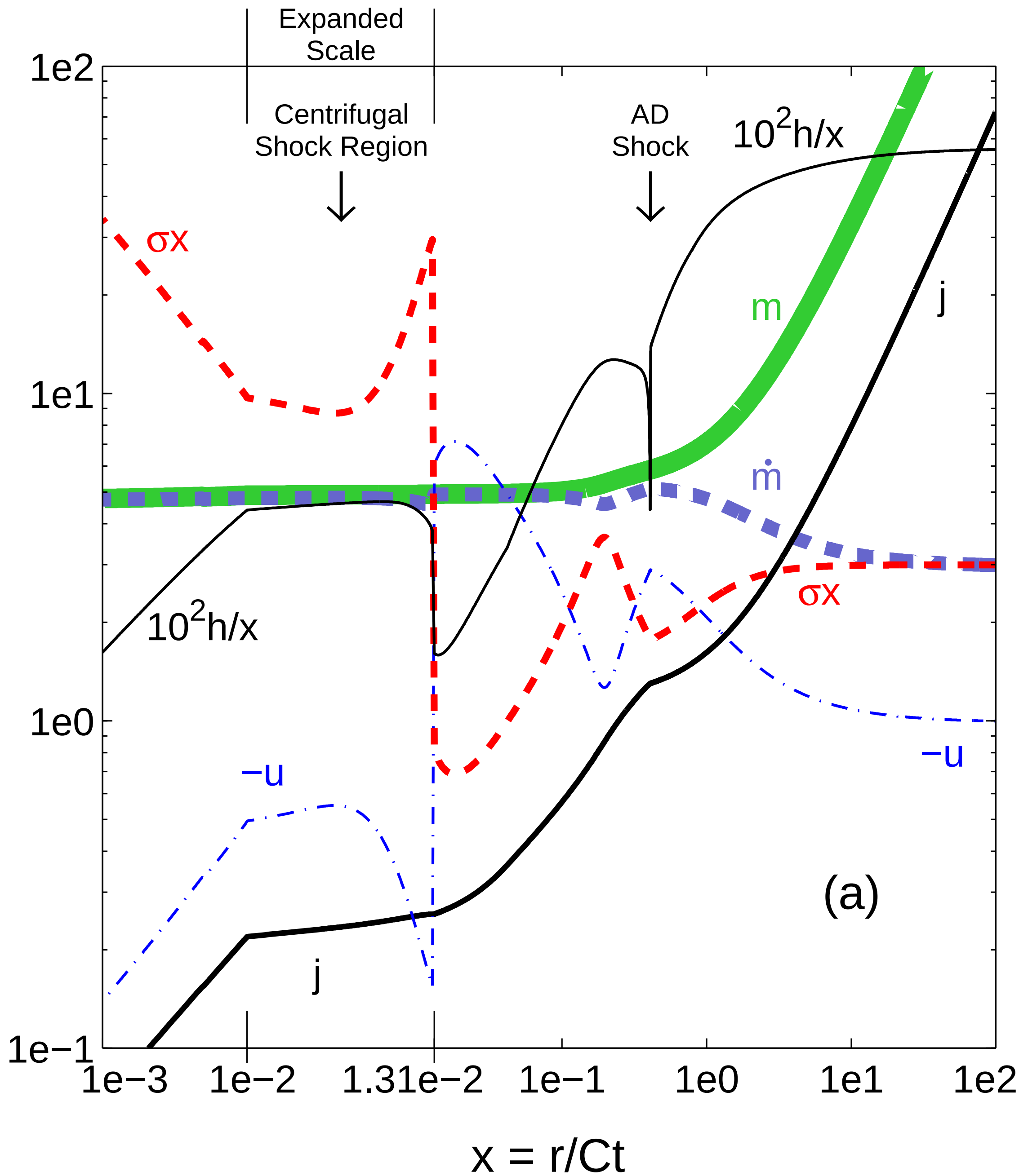


- Outer region ($x > x_\mathrm{a}$): Ideal-MHD infall.
- AD shock—resolved as a continuous transition.
- AD-dominated infall ($x_\mathrm{c} < x < x_\mathrm{a}$): near free-fall controlled by central gravity.
- Centrifugal shock — its location depends sensitively on the diffusivity parameter.
- Keplerian disk ($x < x_\mathrm{c}$) — at any given time, it satisfies $\dot{M}_\mathrm{in}(r) = const$, $B \propto r^{-5/4}$, $B_{r,\mathrm{s}}/B_z = 4/3$ ($r \to 0$ solution).

- ⋆ The asymptotic disk solution implies a significant surface field-line inclination to the rotation axis (nominally $\theta_{\rm s} \approx 53^\circ$), indicating the likelihood of centrifugally driven winds.

- ⋆ The steady-state, radially self-similar disk-wind solution of Blandford & Payne (1982) can be naturally incorporated into this solution since $B \propto r^{-5/4}$ in both cases.

- ⋆ When interpreted in this fashion, the asymptotic solution is found to correspond to a weakly coupled disk/wind configuration.

- ⋆ One can use this model to examine the full range of expected behaviors of real systems — including the limiting cases of (i) fast core rotation and (ii) strong magnetic braking — and study their dependence on the physical parameters.

- ⋆ New insights into the disk formation problem are now starting to be provided by 3D, nonideal-MHD, nested-grid simulations (e.g., Machida et al. 2006).

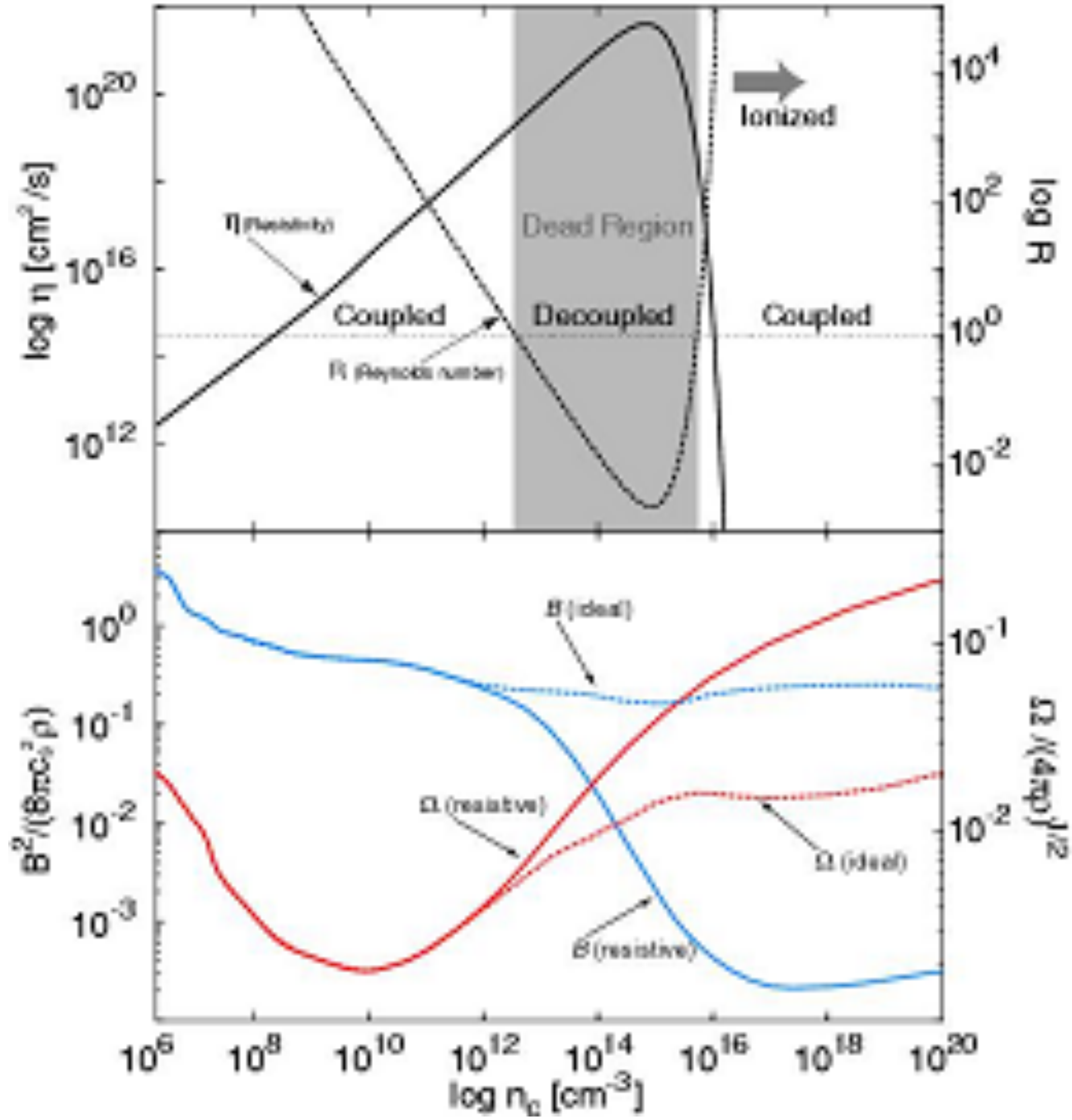

Ionized
Dead Region
Coupled
Decoupled
Coupled
log η [cm²/s]
log R
10^20
10^16
10^12
10^4
10^2
10^0
10^-2
B (ideal)
Ω (resistive)
Ω (ideal)
B (resistive)
B²/(8πc_s²ρ)
Ω /(4πρ)^1/2
10^0
10^-1
10^-2
10^-3
10^6 10^8 10^10 10^12 10^14 10^16 10^18 10^20
log n_c [cm^-3]


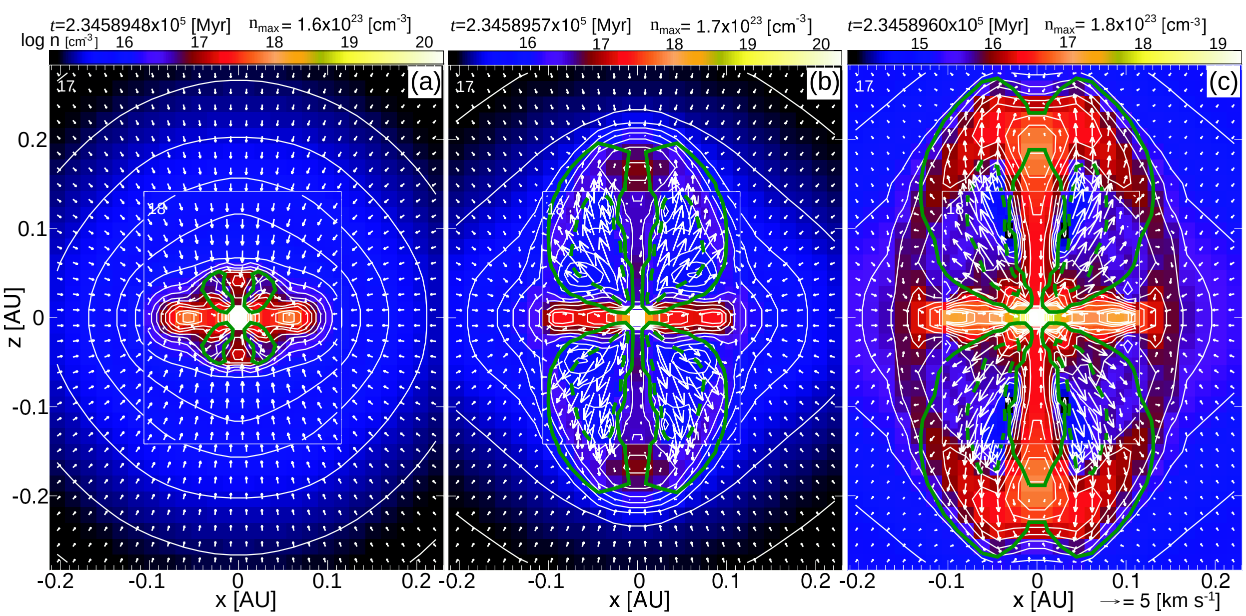

t=2.3458948x10^5 [Myr] n_max= 1.6x10^23 [cm^-3]
log n [cm^-3] 16 17 18 19 20
(a)
t=2.3458957x10^5 [Myr] n_max= 1.7x10^23 [cm^-3]
16 17 18 19 20
(b)
t=2.3458960x10^5 [Myr] n_max= 1.8x10^23 [cm^-3]
15 16 17 18 19
(c)
z [AU]
0.2
0.1
0
-0.1
-0.2
-0.2 -0.1 0 0.1 0.2
x [AU]
→= 5 [km s^-1]

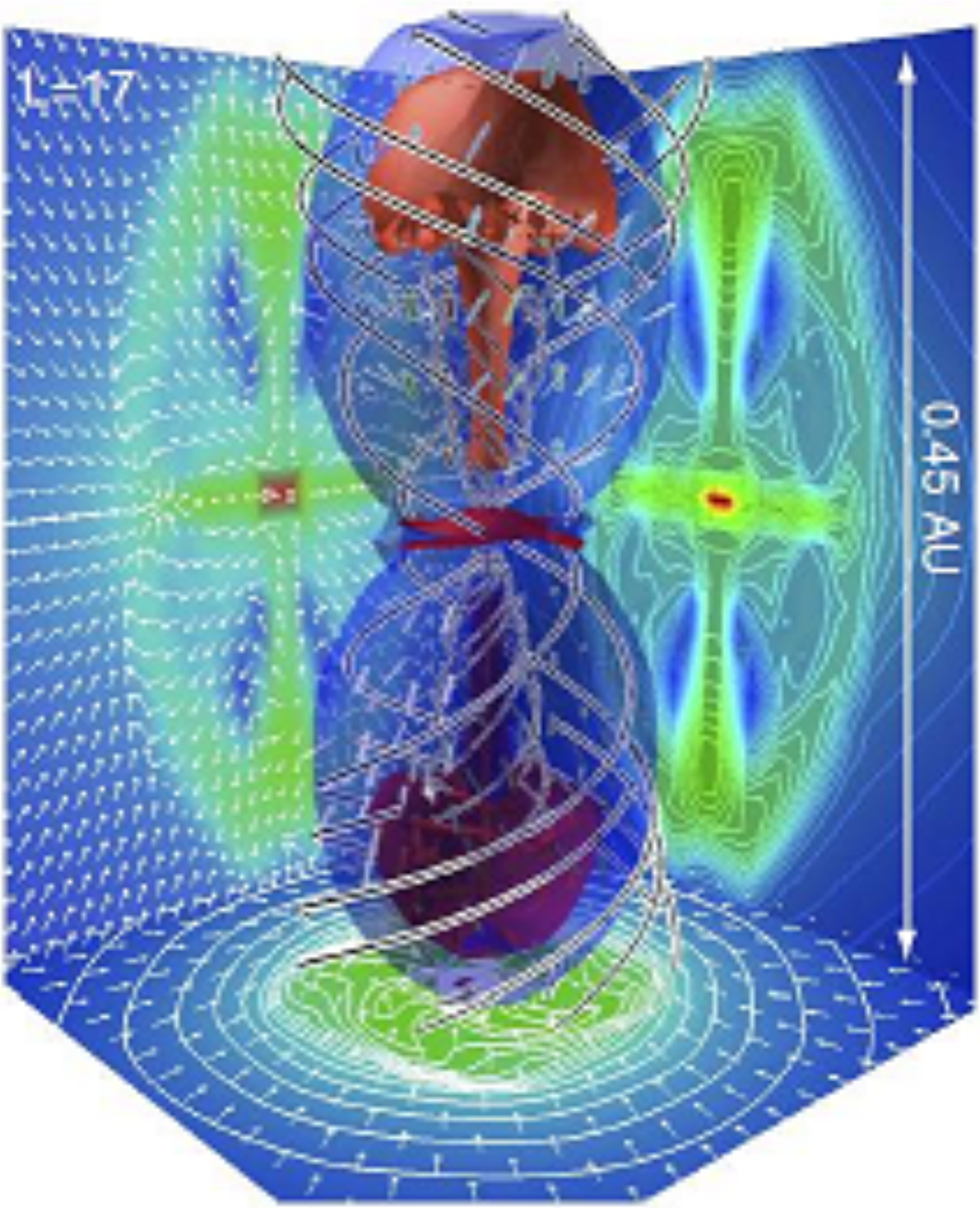


Machida et al. (2006)